UVCS/SOHO spectroscopic observation of Doppler shift oscillations in the solar corona

Mancuso S.[1] and Raymond J. C.[2]

[1]Osservatorio Astrofisico di Torino (OATo, INAF), Torino, Italy

[2]Harvard-Smithsonian Center for Astrophysics, Cambridge, Massachusetts, USA

Harvard – Smithsonian Center for Astrophysics

60 Garden Street, Cambridge, MA 02138

Abstract

We report the discovery of Doppler shift oscillations detected in the H I Ly α (1215.67 Å) coronal emission line with the Ultraviolet Coronagraph Spectrometer (UVCS) onboard SOHO. The UV spectral data were collected at 1.43 $R_\odot$ above the eastern limb of the Sun during a special day-long, high-cadence (20 s) sit-and-stare observation on 1997 December 14. Lomb-Scargle periodogram and wavelet analysis clearly show highly significant Doppler shift oscillations around 14 minutes lasting for several cycles. The cause and nature of these oscillations is still unclear but could be linked to the propagation of a narrow, probably helical CME structure observed a few hours later with the LASCO C2 and C3 coronographs aboard SOHO.

1. Introduction

The H I Lyα (1215.67 Å) data analyzed in this work were collected on 1997 December 14 during a special sit-and-stare observation with the Ultraviolet Coronagraph Spectrometer (UVCS; Kohl et al. 1995). The UVCS slit was centered over the East limb (see Fig. 1) at a radius of 1.43 $R_\odot$ extending from polar angle 74° to 107°. The data were binned to 14" along the 868" slit length with a spectral resolution of 0.14 Å per pixel in the dispersion direction. The observation analyzed in this work began at 15:08 UT and ended on the same day at 21:18 UT and were unique for the very high cadence of the exposures (20 s each).

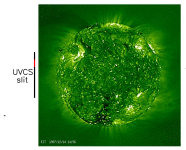

Figure 1. *EIT 195 Å wavelet-enhanced image of the Sun on 1997 December 14. The slit's position at 1.43 $R_\odot$ used for the UVCS observations analyzed in this work is also shown in black. The red portion of the slit shows the angular positions were the significant Doppler shift oscillations were detected.*

The observational data used in this study are the Doppler shift, the intensity, and the width of the H I Lyα coronal emission line at a fixed slit position in the corona, as functions of time. A nonlinear least-squares fit to a Gaussian curve yielded an estimate of the 3 above parameters at each spatial position along the slit. To look for possible periodicities and ascertain their significances, we used 2 methods:
a) the **Lomb-Scargle periodogram** (LSP; Lomb 1976; Scargle 1982) technique, which presents information of possible periodicities by considering the entire data set.
b) the **wavelet transform**, yielding information on periodicity as a function of time.

2. Data analysis

The LSP technique is a widespread tool for the time series analysis of unevenly spaced data allowing for a robust estimation of the statistical significance of each spectral peak. We performed a global analysis of the periods computing the LSP of the 3 parameters at all positions along the slit and with different spatial integrations (that is, by binning the data over several pixels). Apart from a ~5.6° region around position angle 81.1° (plotted in red in Fig. 1), we always found statistical significances < 99%. Fig. 2 shows the LSP computed from the Doppler shift time series plotted in Fig. 3a, obtained by integrating the emission over the selected slit portion. A very significant oscillation is present with a period of about 14.3 ± 0.4 min. The presence of the period is established at a confidence of above the 99.9% significance level.

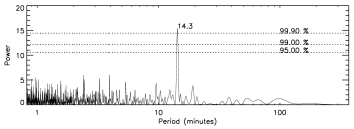

Figure 2. *Lomb Scargle periodogram computed from the Doppler shift time series integrated over the portion of the slit shown in red in Fig. 1. Dotted lines indicate 95%, 99% and 99.9% white-noise significance levels. The most significant period (>99.9% c.l.) is 14.3 ± 0.4 min FWHM.*

In general, coronal time series do not show stationarity: oscillations usually have a finite lifetime or may show a damped or growing character. As a consequence, Fourier spectral methods are of limited use. *Wavelet analysis* provides localized information on a time series in both time and frequency domains by decomposing the series using scaled and translated versions of a wavelet basis function (e.g., Torrence & Compo 1998). The result is a 2D time-frequency image, yielding information on the time-varying amplitude of any periodic signals within the series. Morlet wavelets, used in this work, represent the best compromise between frequency and time localization. In order to use the wavelet technique, the data have been assumed to be uniformly distributed at regular steps with a sample interval of $\Delta t = 24.65$ sec (the original data were irregularly sampled with $\Delta t = 24$, 25 and 26 sec). Fig. 3c displays the power of the wavelet transform for the Doppler shift time series presented in Fig. 3a. The wavelet power spectrum was also averaged over time for comparison with classical spectral methods thus obtaining the *global wavelet power spectrum* (GWS; Fig. 3d). The scale-average wavelet power, shown in Fig. 3(e) is a time series of the average variance in the 13- to 15-min band, and clearly shows how wavelet power is significant (above 95% c.l.) and changes with time within the band.

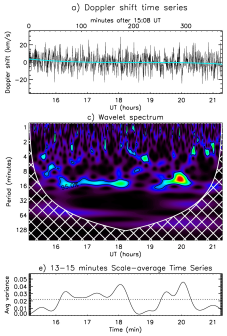

Figure 3.
(a) *Doppler shift time series of the portion of the slit around 81.1°. The colored line superimposed to the graph is a 3rd order polynomial fit that was subtracted prior to analysis.*
(b) *H I Lyα spectral line averaged over all the observation.*
(c) *Wavelet power spectrum using the Morlet mother wavelet.*
(d) *Global wavelet power spectrum. The dotted line is the 95% significance level.*
(e) *Scale-average wavelet power over the 13- to 15-min band. The dashed line is the 95% significance level.*

The wavelet analysis (Fig. 3c) clearly shows a highly significant and stable oscillation around 14 min lasting at least 2 hours (that is, about 8 oscillations) after 16 UT. It fades at around 18:20 UT and shows up again (at about the same frequency) after 19 UT lasting for another hour or so (about 4 oscillations).

In Fig. 4, we show an 11-point moving average applied to the detrended original time series together with a reconstruction of the most significant oscillation obtained with the Singular Spectrum Analysis (SSA) technique, a non-parametric spectral estimation method applied in the time domain that looks for autocovariance patterns in a matrix of lagged copies of a single time series (e.g., Vautard & Ghil 1989). SSA has the ability to decompose a time series into a number of data-adaptive components with simpler structures, such as a slowly varying trend, oscillations and noise. The so-called reconstructed components (RCs) represent the signal of interest in the time domain and the sum of all RCs returns the original time series. Application of the technique to the Doppler shift time series under study yields a dominant oscillation around 14 min (the peak is significant above the 99.9% level). The reconstructed, significant and clearly periodic component is shown in Fig. 4 and nicely agrees (in spectral power) with the wavelet spectrum around 14 min.

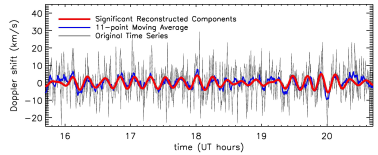

Figure 4. *Doppler shift time series detrended with a 3rd order polynomial. Superimposed to the data, we show an 11-point moving average (blue) and a SSA reconstruction (red) of the most significant oscillation. The reconstruction can be considered as a filtered time series, where the filtering is data adaptive.*

3. Preliminary Results

The nature of the observed Doppler shift oscillations is still unclear but its origin could be linked to a narrow CME structure, propagating at ~ 300 km/s, which we discovered a few hours later higher up in the corona by careful analysis of LASCO C2 and C3 coronograph images (Fig. 5). A flare was also detected by GOES around 16 UT (Fig. 6) but it was probably unrelated to the present event since it occurred near the west limb. During the 1996–97 activity minimum, LASCO recorded several jet-like ejections propagating outward from the Sun's polar regions (St. Cyr et al. 1997; Wang et al. 1998). Subsequent observation near sunspot maximum (Wang & Sheeley 2002) revealed that these jets had angular widths of ~ 3-7° and were distributed over a much greater range of latitudes. Many of them were found to be *recurrent* (from hours to days) and originating from active regions located near the boundaries of non-polar coronal holes. Indeed, a jet-like coronal structure ejected at an angle compatible with the narrow CME observed later with LASCO C2 and C3 is visible in a LASCO C1 difference image obtained a few hours before (Fig. 7).

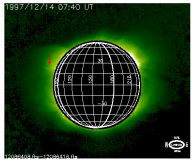

Figure 7. *LASCO C1 difference image showing (indicated by a red arrow) the emission of a collimated jet at 7:40 UT on 1997 December 14.*

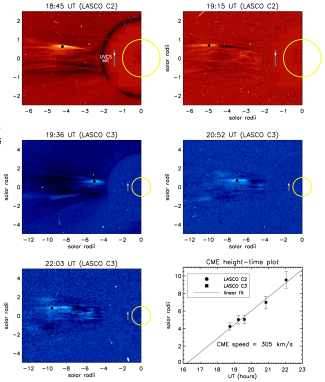

Figure 5. *LASCO C2 and C3 difference images of the narrow CME on 1997 December 14. The images show the CME evolution at 18:48, 19:28 and 20:43 UT.*

These jet-like ejections have also been detected in O VI and H I Lyα by UVCS (e.g., Dobrzycha et al. 2003) and are thought to be triggered by field reconnection between a magnetic dipole and neighboring unipolar region (Wang et al. 1998). More recent stereoscopic observation of polar coronal jets made by the EUVI/SECCHI imagers on board the twin STEREO spacecraft showed evidence of helical structures in polar jets (e.g., Patsourakos et al. 2008) supporting the Pariat et al. (2009) model, in which jets are driven by magnetic untwisting, that predicts the development of a helical structure.

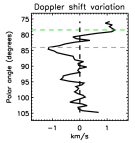

Figure 8. *Doppler shift variation along the slit obtained by comparing 80 min of data taken during the longest oscillation (about 16:30 to 17:50 UT) with 80 min of reference data obtained a few hours before, when the corona was not yet perturbed by the propagation of the narrow CME seen in LASCO C2 and C3 images.*

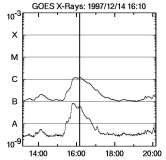

Figure 6. *GOES X-ray flare observed around the onset of the CME. In the SGD reports, the C12 flare was attributed to active region NOAA 8122 located at N29 W41, far away from the eastern limb.*

If a *propagating helical structure* is responsible for the observed Doppler shift oscillation, net Doppler shifts of different signs (when compared to averaged observations taken just before the passage of the helical structure) should be detectable in the upper and lower portions of the slit were the emission was integrated. Indeed, a preliminary analysis shows that this is the case (Fig. 8). We however remark that although the interpretation of the observed Doppler shift oscillations as due to the propagation of a jet-like helical structure seems the most plausible according to our preliminary analysis, other possible interpretations are still viable. Among them, possible candidates are *coronal loop oscillations* (see the large loop structure visible in the wavelet-enhanced EIT image in Fig. 1) and *coronal kink oscillations* of background streamer or current sheet structures, both possibly excited by the jet-like ejection visible in the LASCO images. Subsequent analysis will allow to pinpoint the actual nature of the observed Doppler shift observations.

References

Dobrzycka, D., Raymond, J. C., Biesecker, D. A., Li, J., & Ciaravella, A. 2003, ApJ, 588, 586
Kohl, J. L., et al. 1995, Sol. Phys., 162, 313
Lomb, N. R. 1976, Ap&SS, 39, 447
Pariat, E., Antiochos, S. K., & DeVore, C. R. 2009, ApJ, 691, 61
Patsourakos, S., Pariat, E., Vourlidas, A., Antiochos, S. K., & Wuelser, J. P. 2008, ApJL, 680, L73
Scargle, J. D. 1982, ApJ, 263, 835
St. Cyr, O. C., et al. 1997, in Proc. 31st ESLAB Symp. (ESA SP-415; Noordwijk: ESA), 103
Torrence, C., G. P. Compo, 1998, Bull. Amer. Meteor. Soc., 79, 61
Vautard, R., and M. Ghil 1989, Physica D, 35, 395
Wang, Y.-M., & Sheeley, Jr., N. R. 2002, ApJ, 575, 542
Wang, Y.-M., et al. 1998, ApJ, 508, 899